
On Large-Batch Training for Deep Learning: Generalization Gap and Sharp Minima

Nitish Shirish Keskar*
Northwestern University
Evanston, IL 60208
keskar.nitish@u.northwestern.edu

Dheevatsa Mudigere
Intel Corporation
Bangalore, India
dheevatsa.mudigere@intel.com

Jorge Nocedal
Northwestern University
Evanston, IL 60208
j-nocedal@northwestern.edu

Mikhail Smelyanskiy
Intel Corporation
Santa Clara, CA 95054
mikhail.smelyanskiy@intel.com

Ping Tak Peter Tang
Intel Corporation
Santa Clara, CA 95054
peter.tang@intel.com

Abstract

The stochastic gradient descent method and its variants are algorithms of choice for many Deep Learning tasks. These methods operate in a small-batch regime wherein a fraction of the training data, usually 32–512 data points, is sampled to compute an approximation to the gradient. It has been observed in practice that when using a larger batch there is a significant degradation in the quality of the model, as measured by its ability to generalize. There have been some attempts to investigate the cause for this generalization drop in the large-batch regime, however the precise answer for this phenomenon is, hitherto unknown. In this paper, we present ample numerical evidence that supports the view that large-batch methods tend to converge to sharp minimizers of the training and testing functions – and that sharp minima lead to poorer generalization. In contrast, small-batch methods consistently converge to flat minimizers, and our experiments support a commonly held view that this is due to the inherent noise in the gradient estimation. We also discuss several empirical strategies that help large-batch methods eliminate the generalization gap and conclude with a set of future research ideas and open questions.

1 Introduction

Deep Learning has emerged as one of the cornerstones of large-scale machine learning. Deep Learning models are used for achieving state-of-the-art results on a wide variety of tasks including Computer Vision [25, 37], Natural Language Processing [17, 20] and Reinforcement Learning [31]. The problem of training these networks is one of non-convex optimization. Mathematically, this can be represented as:

*Work was performed when author was an intern at Intel Corporation

$$\min_{x \in \mathbb{R}^n} f(x) := \frac{1}{M} \sum_{i=1}^M f_i(x) \quad (1)$$

where f_i is a loss function for data point $i \in \{1, 2, \dots, M\}$ which captures the deviation of the model prediction with the data, and x is the vector of weights being optimized. The process of optimizing this function is also popularly called *training* of the network. Stochastic Gradient Descent (SGD) [5, 41] and its variants are often used for training deep networks. Generically, these methods minimize the objective function f by iteratively taking steps of the form:

$$x_{k+1} = x_k - \alpha_k \left(\frac{1}{|B_k|} \sum_{i \in B_k} \nabla f_i(x_k) \right) \quad (2)$$

where B_k is the batch sampled from the data set and α_k is the step size at step k . These methods can be interpreted as gradient descent using noisy gradients [4], often referred to as mini-batch gradients with batch size $|B_k|$. SGD and its variants are typically employed in a small-batch regime where $|B_k| \ll M$ and often, $|B_k| \in \{32, 64, \dots, 512\}$. These configurations have been successfully used in practice for a large number of applications; see e.g. [25, 37, 17, 20, 32, 42]. Many strong theoretical properties of these methods are known. These include guarantees of: (a) convergence to minimizers of strong-convex functions and to stationary points for non-convex functions [4], (b) saddle-point avoidance [14, 29], and (c) robustness to input data [18].

However, these methods have a major drawback: owing to the sequential nature of the method and small batch sizes there is limited avenue for parallelization. While some efforts have been made to parallelize SGD [11, 10, 45, 35, 43], the speed-ups and scalability obtained are often limited by the low batch sizes. One natural avenue for increasing parallelism is to increase the batch size B_k . This increases the amount of computation per iteration which can be effectively distributed. However, many practitioners have observed that this leads to a significant loss in generalization performance; see e.g. [28]. In other words, the performance of the model on testing data sets is often worse when trained with large-batch methods as compared to small-batch methods. In our experiments, we have found the drop in generalization (also called generalization gap) to be as high as 5% even for smaller networks.

In this paper, we present numerical results that shed light into this generalization gap. We observe that this gap is explained through the marked sharpness of the minimizers obtained through large-batch methods. The exploration of this drawback of large-batch methods motivate efforts at remedying the generalization problem; the success of such a strategy would have significant ramifications. Indeed, a training algorithm that leverages large batches, without sacrificing generalization performance, would have the implicit ability to scale to a much larger number of nodes as is possible today and could potentially reduce the training time by orders-of-magnitude. We present an idealized performance model in the Appendix C to demonstrate this claim. We emphasize that the goal of our work is not to assess the computation — batch-size trade-off but rather to explore the reasons for the poor performance of large-batch methods for deep learning. To this end, in all our experiments, we place no computational or time budget on the training of networks.

The paper is organized as follows. In the paragraph below, we set the notation used in this paper, in Section 2, we present, our main findings and their supporting numerical evidence. In Section 4, we present some attempts to overcome the problems of large-batch training. Finally, in Section 5 we briefly discuss the relationship between our results and theoretical work [9, 38, 40, 29]. We conclude with open questions concerning the explanation of the generalization gap and possible modifications to make large-batch training viable.

1.1 Notation

As mentioned above, we use the notation f_i to denote the loss function corresponding to the i^{th} data point. The vector of weights is denoted by x and is subscripted by k to denote an iteration. We use the term small-batch (SB) method to denote SGD, or one of its variants like ADAM [23] and ADAGRAD [12], with the proviso that gradient approximation is based on a small mini-batch. In our setup, the size of the batch B_k is fixed for every iteration and is randomly sampled. We use the term large-batch (LB) method to denote any training algorithm like L-BFGS or ADAM that uses a large

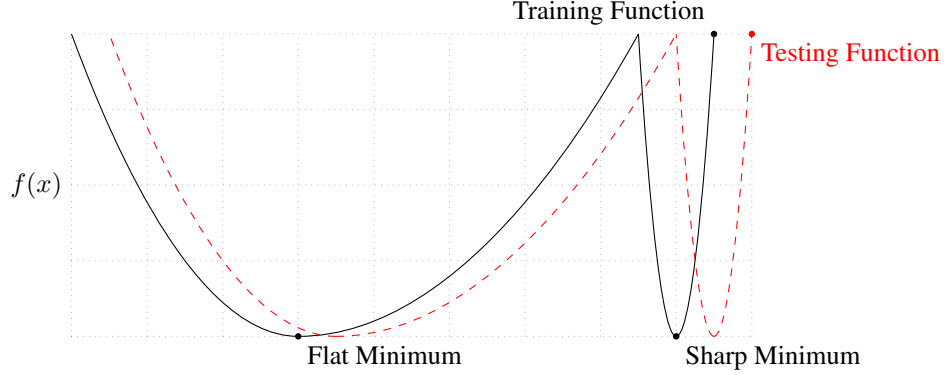


Figure 1: A Conceptual Sketch of Flat and Sharp Minimizers (Y-axis indicates value of the loss function and X-axis indicates the weights)

mini-batch. In our experiments ADAM will be used to illustrate the behavior of both a small or a large batch method.

2 Drawbacks of Large-Batch Methods

2.1 Our Main Observation

As mentioned in Section 1, numerous practitioners have observed a generalization gap when using large-batch methods for training deep learning models. Interestingly, this is despite the fact that large-batch methods usually yield a similar value of the training function as small-batch methods. One may put forth the following as possible causes for this phenomenon: (i) LB methods over-fit the model relative to SB methods, (ii) LB methods lack the *explorative* properties of SB methods and tend to *zoom-in* on the minimizer closest to the initial point, (iii) SB and LB methods converge to qualitatively different minimizers with differing generalization properties, (iv) a minimum number of steps/iterations are necessary for good generalization for an objective function as complex as deep neural networks and due to their computational cost, one cannot perform as many iterations as in a SB method, and (v) LB methods converge to saddle points. The data presented in this paper strongly supports the second and third conjectures².

The main observation of this paper is as follows:

The lack of generalization ability is due to the fact that large-batch methods tend to converge to *sharp minimizers* of the training function. These minimizers are characterized by large positive eigenvalues in $\nabla^2 f(x)$ and tend to generalize less well. In contrast, small-batch methods converge to flat minimizers characterized by small positive eigenvalues of $\nabla^2 f(x)$. We have observed that the loss function landscape of deep neural networks is such that large-batch methods are almost invariably attracted to regions with sharp minima and that, unlike small batch methods, are unable to escape basins of these minimizers.

The observation above clarifies the sharpness of the minimizers that the two regimes (SB and LB) converge to. A large sensitivity in the parameter space has direct consequences on the ability of the trained model to generalize on new data. In this case, the training loss would be low but the generalization error would be high; see Figure 1 for an idealized illustration of this scenario.

In [6], the authors define notions for stability of learning algorithms and use these definitions to prove generalization bounds. In [18], the authors show that for pure-SGD (i.e., with $|B_k| = 1$ for all k), the solution is stable in terms of the uniform stability notion of [6], thus implying generalization. This is true irrespective of the sampling order, and also when employed for a finite number of passes over the data set. Further, the authors state that they were unable to prove any reasonable form of stability

²We cite personal communication with Yann LeCun for these conjectures.

for large-batch gradient descent, and that lower bounds for this approach are necessary before ruling its viability for non-convex machine learning.

The sharpness of a minimizer can be best characterized by the magnitude of the eigenvalues of $\nabla^2 f(x)$, however, given the prohibitive cost of computation in large deep learning applications, we propose a metric which is computationally feasible, even for large networks. The underlying idea is to search for the worst-case loss function value in a small vicinity of the current solution; we discuss this metric in detail in Section 2.2.2.

2.2 Numerical Experiments

In this section, we present numerical evidence to justify the observations made above. To this end, we make use of the visualization technique proposed by [16] and a proposed metric of sharpness (Equation (3)). We consider 6 multi-class classification network configurations for our experiments; they are described in Table 1. The details about the data sets and network configurations are presented in Appendices A and B respectively. As is common for such problems, we use the mean cross entropy loss as the objective function f .

Table 1: Network Configurations

Network Name	Network Type	Architecture	Dataset
F_1	Fully Connected	Section B.1	MNIST [26]
F_2	Fully Connected	Section B.2	TIMIT [13]
C_1	(Shallow) Convolutional	Section B.3	CIFAR-10 [24]
C_2	(Deep) Convolutional	Section B.4	CIFAR-10
C_3	(Shallow) Convolutional	Section B.3	CIFAR-100 [24]
C_4	(Deep) Convolutional	Section B.4	CIFAR-100

The networks were chosen to exemplify popular configurations used in practice like AlexNet [25] and VGGNet [37]. Results on other networks (including LeNet[26] and ResNet[19]) and using other initialization strategies, activation functions, and data sets (such as SVHN [33]) had identical behavior. Since the goal of our work is not to achieve state-of-the-art accuracy or time-to-solution on these tasks but rather to characterize the *nature* of the minima for LB and SB methods, we only describe the final testing accuracy in the main paper and ignore convergence trends.

For all experiments, we used 10% of the training data as batch size for the large-batch experiments and 256 for small-batch experiments. We used the ADAM optimizer for either regime. Experiments with other optimizers for the large-batch experiments, including ADAGRAD [12], SGD[41] and adaQN [22], led to similar results. All experiments were conducted 5 times from different (uniformly distributed random) starting points to prevent issues of spurious starting points and we report both mean and standard-deviations of measured quantities. The baseline performance for our setup is presented Table 2. We can observe from the Table 2 that on all networks, both approaches led to high training accuracy but there is a statistically significant difference in the generalization performance.

Further, the networks were trained, without any budget or limits, till the loss function saturated. We emphasize that the generalization gap is not due to *over-fitting* as commonly observed in statistics. Over-fitting, in this sense, is caused by excessive training of an over-represented model on the available data and manifests itself in the form of a testing accuracy curve which, at a certain iterate peaks, and then decays due to the model learning idiosyncrasies of the training data. This is not what we observe in our experiments; see Figure 2 for the training–testing curve on the representative F_2 and C_1 networks; we omit the results on other network for brevity. As such, early-stopping heuristics aimed at preventing models from over-fitting would not help reduce the generalization gap. The difference between the *training and testing* accuracies for the networks arises due to the specific choice of the network (e.g. AlexNet, VGGNet etc.) and is not the focus of this study, as we mention above. Rather, our goal is to study the source of the testing performance disparity of the two regimes (SB and LB) on a given network model.

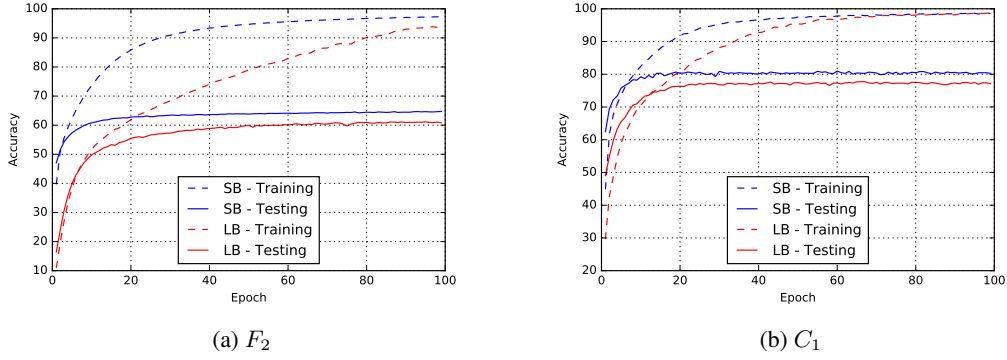


Figure 2: Convergence trajectories of training and testing accuracy for SB and LB methods

Table 2: Performance of small-batch (SB) and large-batch (LB) variants of ADAM on the 6 networks listed in Table 1

Network Name	Training Accuracy		Testing Accuracy	
	SB	LB	SB	LB
F_1	$99.66\% \pm 0.05\%$	$99.92\% \pm 0.01\%$	$98.03\% \pm 0.07\%$	$97.81\% \pm 0.07\%$
F_2	$99.99\% \pm 0.03\%$	$98.35\% \pm 2.08\%$	$64.02\% \pm 0.2\%$	$59.45\% \pm 1.05\%$
C_1	$99.89\% \pm 0.02\%$	$99.66\% \pm 0.2\%$	$80.04\% \pm 0.12\%$	$77.26\% \pm 0.42\%$
C_2	$99.99\% \pm 0.04\%$	$99.99 \pm 0.01\%$	$89.24\% \pm 0.12\%$	$87.26\% \pm 0.07\%$
C_3	$99.56\% \pm 0.44\%$	$99.88\% \pm 0.30\%$	$49.58\% \pm 0.39\%$	$46.45\% \pm 0.43\%$
C_4	$99.10\% \pm 1.23\%$	$99.57\% \pm 1.84\%$	$63.08\% \pm 0.5\%$	$57.81\% \pm 0.17\%$

2.2.1 Parametric Plots

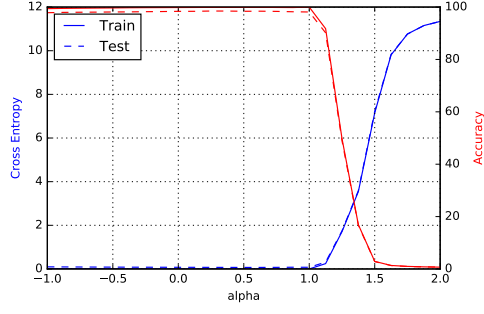
We first present parametric 1-D plots of the function as described in [16]. Let x_s^* and x_ℓ^* indicate the solutions obtained by running ADAM using small and large batch sizes respectively. We plot the loss function, on both training and testing data sets, along the line-segment connecting the two points. For $\alpha \in [0, 2]$, we plot the function $f(\alpha x_\ell^* + (1 - \alpha)x_s^*)$ and also superimpose the classification accuracy at the intermediate points; see Figure 3³. For this experiment, we randomly chose a pair of minimizers (SB and LB) from the 5 trials used to generate the data in Table 2. The plots show that the LB minima are strikingly sharper than the SB minima in this one-dimensional manifold. The plots in Figure 3 only explore a linear slice of the function. In Figure 4, we present similar plot except we plot $f(\sin(\frac{\alpha\pi}{2})x_\ell^* + \cos(\frac{\alpha\pi}{2})x_s^*)$ to monitor the function along a curved path between the two points. Here too, the relative sharpness of the minima is evident.

2.2.2 Sharpness of Minima and Their Prevalence

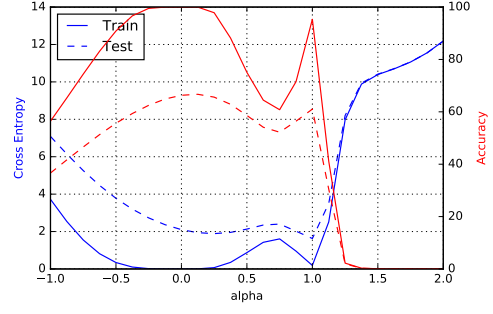
The parametric plots presented in the previous section describe the function along one-dimensional subspaces. These plots, however, do not provide any information about the behavior of the function around the minimizer in the entire space. To further buttress our numerical evidence, we propose, and present values for, a metric for approximating the relative sensitivity of the solution, i.e., sharpness. The general idea is to explore a small neighborhood of a solution and compute the largest value that the function f can attain in that neighborhood and use that to measure the sensitivity. This exploration can be conducted in the whole space or on a smaller dimensional manifold. For the latter we introduce a matrix A , whose columns are randomly generated. The inclusion of the matrix A is motivated by the fact that the worst-case cost can be a quite pessimistic approximation of sensitivity; e.g., if there are only a few high-curvature directions for an otherwise flat minima.

Let C_ϵ denote the neighborhood around the solution that is explored and let $A \in \mathbb{R}^{n \times p}$ denote a sub-sampling matrix whose column-space corresponds to the subspace for optimization. In order to ensure invariance of sharpness to problem dimension, sparsity and scale, we use the constraint set C_ϵ

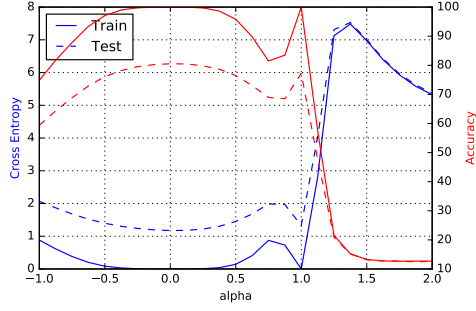
³The code to reproduce the parametric plot on exemplary networks can be found in our GitHub repository: <https://github.com/keskarnitish/large-batch-training>.



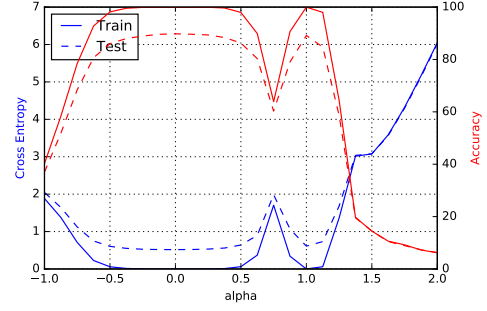
(a) F_1



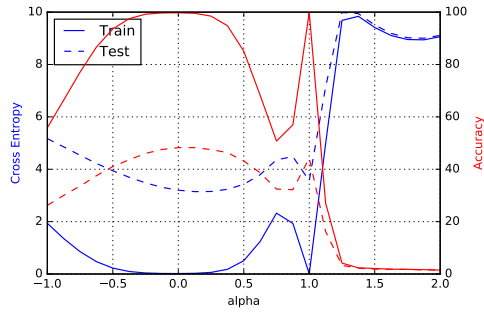
(b) F_2



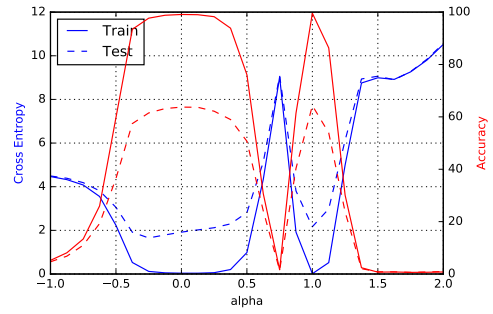
(c) C_1



(d) C_2

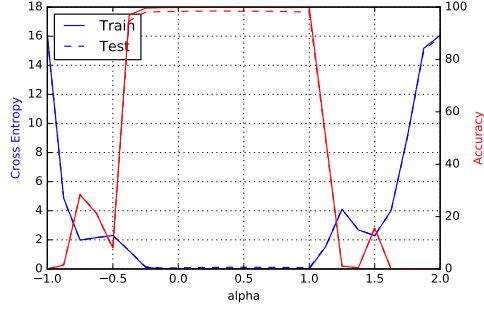


(e) C_3

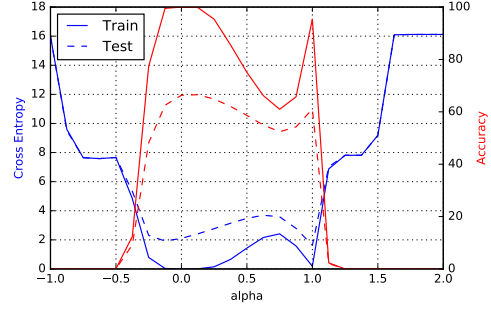


(f) C_4

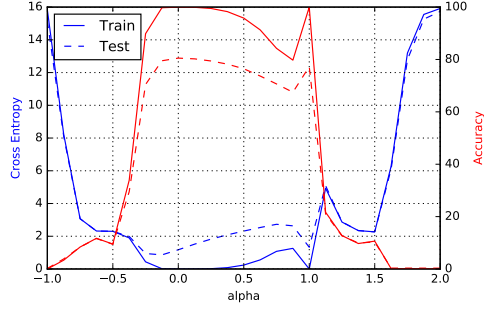
Figure 3: Parametric Plots – Linear (Left axis corresponds to cross-entropy loss, f , and right axis corresponds to classification accuracy; solid line indicates training data set and dashed line indicated testing data set); $\alpha = 0$ corresponds to the SB minimizer while $\alpha = 1$ corresponds to the LB minimizer



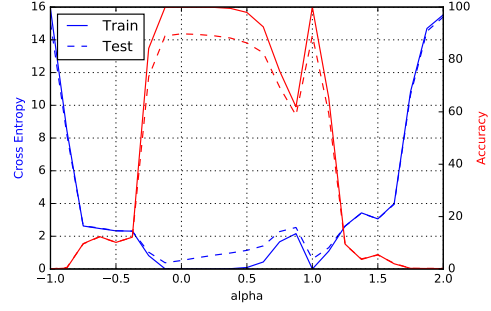
(a) F_1



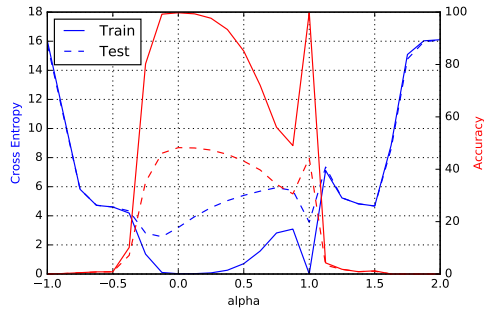
(b) F_2



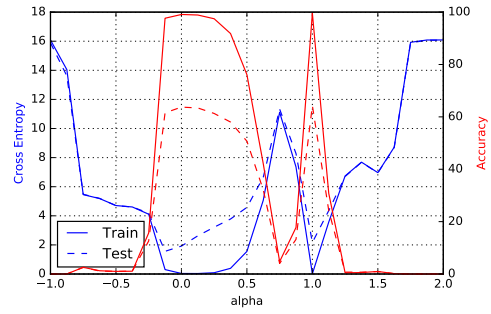
(c) C_1



(d) C_2



(e) C_3



(f) C_4

Figure 4: Parametric Plots – Curvilinear (Left axis corresponds to cross-entropy loss, f , and right axis corresponds to classification accuracy; solid line indicates training data set and dashed line indicated testing data set); $\alpha = 0$ corresponds to the SB minimizer while $\alpha = 1$ corresponds to the LB minimizer

defined as:

$$C_\epsilon = \{z \in \mathbb{R}^p : -\epsilon(|(A^+x)_i| + 1) \leq z_i \leq \epsilon(|(A^+x)_i| + 1) \quad \forall i \in \{1, 2, \dots, p\}\}$$

where A^+ denotes the pseudo-inverse of A .

Metric 2.1. Given a point $x \in \mathbb{R}^n$, $\epsilon > 0$ and $A \in \mathbb{R}^{n \times p}$, we define the (C_ϵ, A) -sharpness of x as:

$$\phi_{x,f}(\epsilon, A) := \frac{(\max_{y \in C_\epsilon} f(x + Ay)) - f(x)}{1 + f(x)} \times 100. \quad (3)$$

Unless specified otherwise, we use this metric for sharpness for the rest of the paper and use the value of this metric and the term *sharpness* interchangeably. Further, if A is not specified, it is assumed to be $I_{n \times n}$.

We present the values of the metric for the minima of the various problems in Tables 3 and 4. The former explores the full-space (i.e., $A = I_n$) while the latter uses a randomly sampled $n \times 100$ dimensional matrix A . We report results with two values of ϵ , $(10^{-3}, 5 \cdot 10^{-4})$. In all experiments, we solve the maximization problem in Equation 3 using L-BFGS-B [8] for 10 iterations.

Table 3: Sharpness of Minima in Full Space

	$\epsilon = 10^{-3}$		$\epsilon = 5 \cdot 10^{-4}$	
	SB	LB	SB	LB
F_1	1.23 ± 0.83	205.14 ± 69.52	0.61 ± 0.27	42.90 ± 17.14
F_2	1.39 ± 0.02	310.64 ± 38.46	0.90 ± 0.05	93.15 ± 6.81
C_1	28.58 ± 3.13	707.23 ± 43.04	7.08 ± 0.88	227.31 ± 23.23
C_2	8.68 ± 1.32	925.32 ± 38.29	2.07 ± 0.86	175.31 ± 18.28
C_3	29.85 ± 5.98	258.75 ± 8.96	8.56 ± 0.99	105.11 ± 13.22
C_4	12.83 ± 3.84	421.84 ± 36.97	4.07 ± 0.87	109.35 ± 16.57

Table 4: Sharpness of Minima in Random Subspace

	$\epsilon = 10^{-3}$		$\epsilon = 5 \cdot 10^{-4}$	
	SB	LB	SB	LB
F_1	0.11 ± 0.00	9.22 ± 0.56	0.05 ± 0.00	9.17 ± 0.14
F_2	0.29 ± 0.02	23.63 ± 0.54	0.05 ± 0.00	6.28 ± 0.19
C_1	2.18 ± 0.23	137.25 ± 21.60	0.71 ± 0.15	29.50 ± 7.48
C_2	0.95 ± 0.34	25.09 ± 2.61	0.31 ± 0.08	5.82 ± 0.52
C_3	17.02 ± 2.20	236.03 ± 31.26	4.03 ± 1.45	86.96 ± 27.39
C_4	6.05 ± 1.13	72.99 ± 10.96	1.89 ± 0.33	19.85 ± 4.12

Both tables show a 1–2 order-of-magnitude difference between the values of our metric for the two regimes. This further reinforces our claim that the large-batch solutions have comparatively larger sensitivity.

3 Success of Small-Batch Methods

It is often reported by practitioners that when increasing the batch size for a problem, there exists a threshold after which there is sharp deterioration in the quality of the model. We present evidence for this claim for the F_2 and C_1 networks in Figure 5. In both of these experiments, there is a batch size (≈ 15000 for F_2 and ≈ 500 for C_1) after which there is a large drop in testing accuracy. Notice also that the upward drift in value of the sharpness is considerably reduced around this threshold. Similar thresholds exist for other networks, which we eliminate for brevity. This experiment also attempts to answer the question *Why do SB methods not converge to sharp minimizers?* as we explain next.

Small-batch methods use stochastic gradients for computing steps, which are noisy versions of the true gradient $\nabla f(x)$. In the basins of sharp minimizers, any noise in the gradient will *push* the iterate out of the basin and encourage movement towards a flatter minimizer where noise will not cause exit from basin. After the aforementioned threshold of batch size is crossed, the noise in the

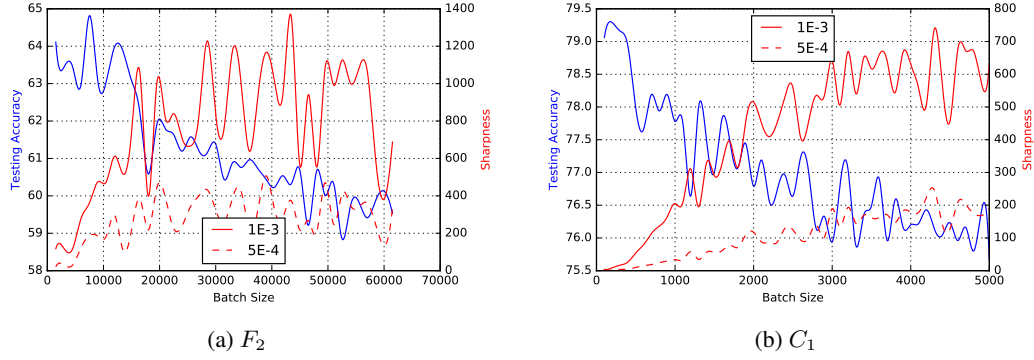


Figure 5: Testing Accuracy and Sharpness v/s Batch Size (X-axis corresponds to the batch size used for training the network for 100 epochs, left Y-axis corresponds to the testing accuracy at the final iterate and right Y-axis corresponds to the sharpness of that iterate)

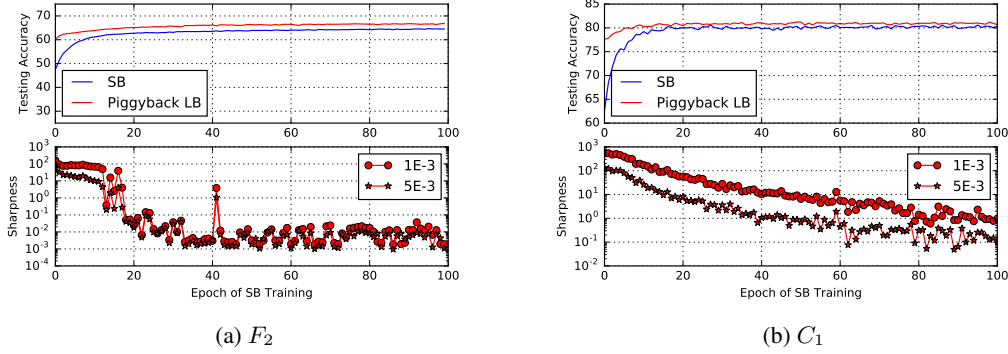


Figure 6: Piggybacking Experiment (X-axis denotes the number of SB training epochs and Y-axis denotes the testing accuracy for: (i) the SB method iterates, and (b) points obtained using current SB iterate as warm-start for a 100-epoch training of the LB method)

stochastic gradient is not sufficient to cause ejection from sharp basins leading to convergence to sharper minimizer

To explore that in more detail, consider the following experiment. We train the network using 0.25% batch size using ADAM for 100 epochs and retain the iterate after each epoch in memory. Using these 100 iterates as starting points and train the network using a LB method for 100 epochs and receive a 100 *piggybacked* (or warm-started) large-batch solutions. We then plot the accuracy and sharpness of large-batch solutions, along with the accuracy of the small-batch solution, in Figure 6.

The results provide additional insights in the behavior of the two regimes. For a few initial epochs, the *piggybacking* of the LB method on the SB method iterates does not cause generalization improvement. This situation is not very different from that of Table 2. The concomitant sharpness of the iterates also stays high. We argue that this is the region wherein the noise is crucial to avoid sharp minima. However, after a threshold, the accuracy improves and sharpness of the large-batch iterates drop. This happens, we then argue, when the SB method has ended its exploration phase and discovered a flat minimizer; the large-batch method is the able to converge towards it leading to comparable testing accuracy.

As mentioned above, it has been speculated that LB methods tend to be attracted to sharp minimizers close to the starting point, whereas SB methods move away and locate minimizers that are farther away; our numerical experiments reinforce this. We observed that the ratio of $\|x_s^* - x_0\|_2$ and $\|x_\ell^* - x_0\|_2$ was in the range of $[3 - 10]$. In order to further test our hypothesis of the effect of noise, we plot the sharpness of the iterates for the two regimes for one random trial of the F_2 and C_1 networks against the loss function (cross entropy) value at that iteration in Figure 7. At larger

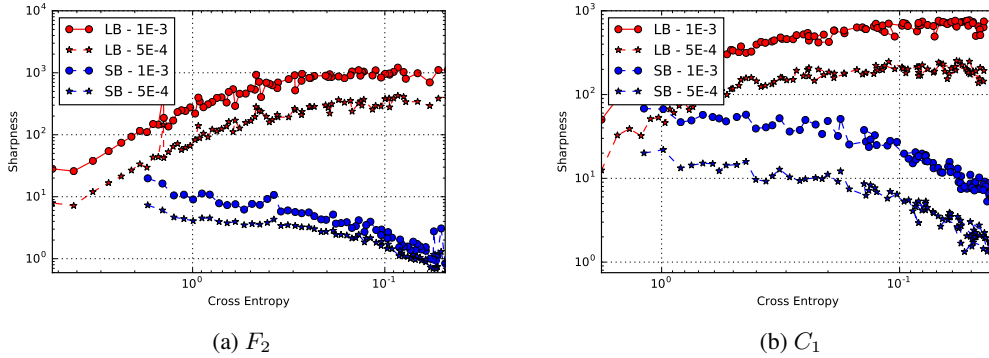


Figure 7: Sharpness v/s Cross Entropy Loss

loss values, i.e. near the initial point, both regimes have similar value of sharpness. However, as the loss function reduces, the value of sharpness for the two regimes have very different behavior. The sharpness of the iterates corresponding to the LB method rapidly increases suggesting convergence to a sharp minimizer. On the other hand, for the SB method the sharpness stays relatively constant and then reduces, suggesting an exploration phase followed by convergence to a flat minimizer. The lack of exploration and the resulting *zooming-in* towards the closest minimizer to the starting point is often quoted as the reason for failure of large-batch methods [28]. However, it is unclear why by itself such *zooming-in* would be detrimental. Our numerical evidence concerning the sharpness of the minima aims to complete this explanation.

4 Attempts to Alleviate the Problem

In this section, we discuss a few strategies that aim to remedy the problem of poor generalization for large-batch methods. As in Section 2, we use 10% as the percentage batch-size for large-batch experiments and 0.25% for small-batch methods. For all experiments, we use ADAM as the optimizer irrespective of batch-size.

4.1 Data Augmentation

Given that large-batch methods appear to be attracted to sharp minimizers, one can ask whether it is possible to modify the geometry of the loss function so that it is more benign to large-batch methods. The loss function depends both on the geometry of the objective function and to the size and properties of the training set. One approach we consider is data augmentation; see e.g. [2, 25, 37]. The application of this technique is domain specific but generally involves augmenting the data set through controlled modifications on the training data. For instance, in the case of image recognition, the training set can be augmented through translations, rotations, shearing and flipping of the training data. This technique leads to regularization of the network and has been employed for improving testing accuracy on several data sets.

In our experiments, we train the 4 image-based (convolutional) networks using aggressive data augmentation and present the results in Table 5. For the augmentation, we use horizontal reflections, random rotations up to 10° and random translation of up to 0.2 times the size of the image. It is evident from the table that, while the LB method achieves accuracy comparable to the SB method (also with training data augmented), the sharpness of the minima still exists, suggesting sensitivity to images contained in neither training or testing set. In this section, we exclude parametric plots and sharpness values for the SB method owing to space constraints and the similarity to those presented in Section 2.2.

Table 5: Effect of Data Augmentation

	Testing Accuracy		Sharpness (LB method)	
	Baseline (SB)	Augmented LB	$\epsilon = 10^{-3}$	$\epsilon = 5 \cdot 10^{-4}$
C_1	$83.63\% \pm 0.14\%$	$82.50\% \pm 0.67\%$	231.77 ± 30.50	45.89 ± 3.83
C_2	$89.82\% \pm 0.12\%$	$90.26\% \pm 1.15\%$	468.65 ± 47.86	105.22 ± 19.57
C_3	$54.55\% \pm 0.44\%$	$53.03\% \pm 0.33\%$	103.68 ± 11.93	37.67 ± 3.46
C_4	$63.05\% \pm 0.5\%$	$65.88 \pm 0.13\%$	271.06 ± 29.69	45.31 ± 5.93

Table 6: Effect of Conservative Training

	Testing Accuracy		Sharpness (LB method)	
	Baseline (SB)	Conservative LB	$\epsilon = 10^{-3}$	$\epsilon = 5 \cdot 10^{-4}$
F_1	$98.03\% \pm 0.07\%$	$98.12\% \pm 0.01\%$	232.25 ± 63.81	46.02 ± 12.58
F_2	$64.02\% \pm 0.2\%$	$61.94\% \pm 1.10\%$	928.40 ± 51.63	190.77 ± 25.33
C_1	$80.04\% \pm 0.12\%$	$78.41\% \pm 0.22\%$	520.34 ± 34.91	171.19 ± 15.13
C_2	$89.24\% \pm 0.05\%$	$88.495\% \pm 0.63\%$	632.01 ± 208.01	108.88 ± 47.36
C_3	$49.58\% \pm 0.39\%$	$45.98\% \pm 0.54\%$	337.92 ± 33.09	110.69 ± 3.88
C_4	$63.08\% \pm 0.10\%$	62.51 ± 0.67	354.94 ± 20.23	68.76 ± 16.29

4.2 Conservative Training

In [30], the authors argue that the convergence rate of SGD for the large-batch setting can be improved by obtaining iterates through the following proximal sub-problem.

$$x_{k+1} = \arg \min_x f_{B_k}(x) + \frac{\lambda}{2} \|x - x_k\|_2^2 \quad (4)$$

Here, f_{B_k} denotes the function defined using the batch B_k , i.e., $f_{B_k}(x) = \frac{1}{|B_k|} \sum_{i \in B_k} f_i(x)$. The motivation of this strategy is, in the context of large-batch methods, to better utilize a batch before moving onto the next one. The problem is solved inexactly using 3–5 iterations of gradient descent, co-ordinate descent or L-BFGS. They show that this not only improves the convergence rate of SGD but also leads to improved empirical performance on convex machine learning problems. The underlying idea of utilizing a batch is not specific to convex problems and we can apply the same framework for deep learning, however, without theoretical guarantees. Indeed, a similar algorithm, was proposed in [43] for Deep Learning albeit but with emphasis on parallelization of small-batch SGD and asynchrony. The results using the conservative training approach are presented in Figure 6. In all experiments, we solve the problem 4 using 3 iterations of ADAM and set the regularization parameter λ to be 10^{-3} . Again, there is a statistically significant improvement in the testing accuracy of the large-batch method but it does not solve the problem of sensitivity.

4.3 Robust Training

A natural way of avoiding sharp minima is through Robust Optimization techniques [1]. These techniques attempt to optimize a worst-case cost as opposed to the nominal (or true) cost. Mathematically, given an $\epsilon > 0$, these techniques optimize the function

$$\min_x \phi(x) := \max_{\|\Delta x\| \leq \epsilon} f(x + \Delta x) \quad (5)$$

Geometrically, classical (nominal) optimization attempts to locate the lowest point of a valley while Robust Optimization attempts to lower an ϵ -disc down the loss surface. We refer an interested reader to [3], and the references therein, for a review of non-convex robust optimization. A direct application of this technique is not feasible since each iteration is prohibitively expensive in our setup since it involves solving a large-scale Second-Order Conic Program (SOCP).

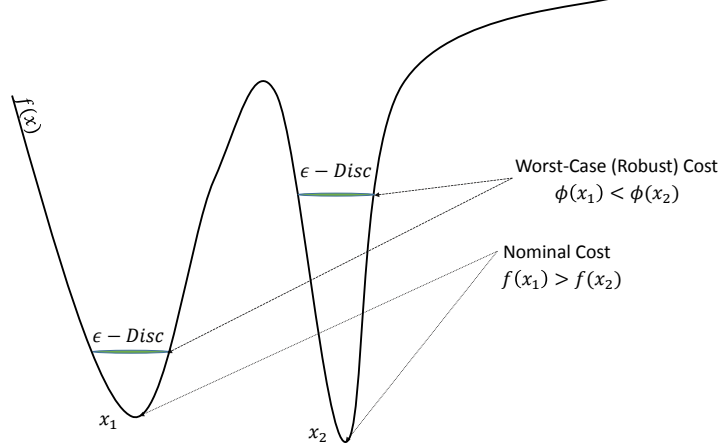


Figure 8: Illustration of Robust Optimization

In the context of Deep Learning, there are two inter-dependent forms of robustness: robustness to the data and robustness to the solution. The former leverages the fact that the function f is inherently a statistical model, while the latter treats f as a black-box function. In [36], the authors show the equivalence between robustness of the solution (with respect to the data) and adversarial training [15].

Given the partial success of the data augmentation strategy, it is natural to question the efficacy of adversarial training. As described in [15], adversarial training also aims to artificially increase the training set but, unlike randomized data augmentation, uses the model’s sensitivity to construct new examples. Despite its intuitive appeal, in our experiments, we found that this strategy did not improve generalization outcomes. Similarly, we received no generalization benefit in stability training proposed by [44]. In both cases, the testing accuracy, sharpness values and the parametric plots were similar to the unmodified (baseline) case discussed in Section 2. It remains to be shown whether adversarial training (or any other form of robust training) can be leveraged to increase the viability of large-batch training.

5 Discussion and Conclusion

In this paper, we present numerical experiments that support the view that the presence of (and convergence to) sharp minimizers is the cause for the poor generalization of large-batch methods for Deep Learning. To this end, we provide evidence in the form of 1-dimensional parametric plots and worst-case perturbation measures for a variety of Deep Learning architectures. Further, we describe our attempts to remedy the problem including data augmentation and conservative training. Our preliminary investigation suggests that these strategies do not completely correct the problem in that they improve the generalization of large-batch methods but still lead to relatively sharp minima. Another prospective remedy includes the use of *dynamic sampling* or switching-based strategy which leverages small batches in the first few epochs and either gradually, or abruptly, transitions into a large-batch method; see e.g. [7]. The potential viability of this approach is suggested by our *piggybacking* experiments (see Figure 6) wherein we achieve competitive testing accuracy using a large-batch method when hot-started with a small-batch inexactly trained network. The possibility of using this and combination of the aforementioned strategies is a topic of future research.

Recently, a number of researchers have described interesting theoretical properties of the loss surface of deep neural networks; see for e.g. [9, 38, 40, 29]. Their work, under regularity assumptions, shows that the loss function of deep learning models is fraught with many local minimizers. However, these majority of these minimizers are shown to be at the similar depth (in terms of loss function). We point out that our results are in alignment these observations since, in our experiments, both sharp and flat minimizers exist at the similar depth. To the best of our knowledge, the relative sharpness and frequency of minimizers on the loss surface remains to be explored theoretically.

Our results encourage open questions: (a) in the light of our observations, can one prove/disprove convergence of large-batch methods to sharp minimizers?; (b) what is the relative density of the two kinds of minima?; (c) can one design neural network architectures for various tasks that account for sensitivity of LB methods?; (d) can the networks be initialized in a way that enables LB methods to succeed?; and (e) is it possible, through algorithmic or regulatory means to steer LB methods away from sharp minimizers?

References

- [1] Aharon Ben-Tal, Laurent El Ghaoui, and Arkadi Nemirovski. *Robust optimization*. Princeton University Press, 2009.
- [2] Yoshua Bengio, Ian Goodfellow, and Aaron Courville. Deep learning. Book in preparation for MIT Press, 2016.
- [3] Dimitris Bertsimas, Omid Nohadani, and Kwong Meng Teo. Robust optimization for unconstrained simulation-based problems. *Operations Research*, 58(1):161–178, 2010.
- [4] Léon Bottou. Online learning and stochastic approximations. *On-line learning in neural networks*, 17(9):142, 1998.
- [5] Léon Bottou. Large-scale machine learning with stochastic gradient descent. In *Proceedings of COMPSTAT’2010*, pages 177–186. Springer, 2010.
- [6] Olivier Bousquet and André Elisseeff. Stability and generalization. *Journal of Machine Learning Research*, 2(Mar):499–526, 2002.
- [7] Richard H Byrd, Gillian M Chin, Jorge Nocedal, and Yuchen Wu. Sample size selection in optimization methods for machine learning. *Mathematical programming*, 134(1):127–155, 2012.
- [8] Richard H Byrd, Peihuang Lu, Jorge Nocedal, and Ciyu Zhu. A limited memory algorithm for bound constrained optimization. *SIAM Journal on Scientific Computing*, 16(5):1190–1208, 1995.
- [9] Anna Choromanska, Mikael Henaff, Michael Mathieu, Gérard Ben Arous, and Yann LeCun. The loss surfaces of multilayer networks. In *AISTATS*, 2015.
- [10] Dipankar Das, Sasikanth Avancha, Dheevatsa Mudigere, Karthikeyan Vaidynathan, Srinivas Sridharan, Dhiraj Kalamkar, Bharat Kaul, and Pradeep Dubey. Distributed deep learning using synchronous stochastic gradient descent. *arXiv preprint arXiv:1602.06709*, 2016.
- [11] Jeffrey Dean, Greg Corrado, Rajat Monga, Kai Chen, Matthieu Devin, Mark Mao, Andrew Senior, Paul Tucker, Ke Yang, Quoc V Le, et al. Large scale distributed deep networks. In *Advances in neural information processing systems*, pages 1223–1231, 2012.
- [12] J. Duchi, E. Hazan, and Y. Singer. Adaptive subgradient methods for online learning and stochastic optimization. *The Journal of Machine Learning Research*, 12:2121–2159, 2011.
- [13] John S Garofolo, Lori F Lamel, William M Fisher, Jonathan G Fiscus, David S Pallett, Nancy L Dahlgren, and Victor Zue. Timit acoustic-phonetic continuous speech corpus. *Linguistic data consortium, Philadelphia*, 33, 1993.
- [14] Rong Ge, Furong Huang, Chi Jin, and Yang Yuan. Escaping from saddle points—online stochastic gradient for tensor decomposition. In *Proceedings of The 28th Conference on Learning Theory*, pages 797–842, 2015.
- [15] Ian J Goodfellow, Jonathon Shlens, and Christian Szegedy. Explaining and harnessing adversarial examples. *arXiv preprint arXiv:1412.6572*, 2014.
- [16] Ian J Goodfellow, Oriol Vinyals, and Andrew M Saxe. Qualitatively characterizing neural network optimization problems. *arXiv preprint arXiv:1412.6544*, 2014.
- [17] Alex Graves, Abdel-rahman Mohamed, and Geoffrey Hinton. Speech recognition with deep recurrent neural networks. In *2013 IEEE international conference on acoustics, speech and signal processing*, pages 6645–6649. IEEE, 2013.
- [18] M. Hardt, B. Recht, and Y. Singer. Train faster, generalize better: Stability of stochastic gradient descent. *arXiv preprint arXiv:1509.01240*, 2015.

- [19] Kaiming He, Xiangyu Zhang, Shaoqing Ren, and Jian Sun. Deep residual learning for image recognition. *arXiv preprint arXiv:1512.03385*, 2015.
- [20] Geoffrey Hinton, Li Deng, Dong Yu, George E Dahl, Abdel-rahman Mohamed, Navdeep Jaitly, Andrew Senior, Vincent Vanhoucke, Patrick Nguyen, Tara N Sainath, et al. Deep neural networks for acoustic modeling in speech recognition: The shared views of four research groups. *IEEE Signal Processing Magazine*, 29(6):82–97, 2012.
- [21] Sergey Ioffe and Christian Szegedy. Batch normalization: Accelerating deep network training by reducing internal covariate shift. *arXiv preprint arXiv:1502.03167*, 2015.
- [22] Nitish Shirish Keskar and Albert S Berahas. adan: An adaptive quasi-newton algorithm for training rnns. *arXiv preprint arXiv:1511.01169*, 2015.
- [23] D. Kingma and J. Ba. Adam: A method for stochastic optimization. In *International Conference on Learning Representations (ICLR 2015)*, 2015.
- [24] Alex Krizhevsky and Geoffrey Hinton. Learning multiple layers of features from tiny images. 2009.
- [25] Alex Krizhevsky, Ilya Sutskever, and Geoffrey E Hinton. Imagenet classification with deep convolutional neural networks. In *Advances in neural information processing systems*, pages 1097–1105, 2012.
- [26] Yann LeCun, Léon Bottou, Yoshua Bengio, and Patrick Haffner. Gradient-based learning applied to document recognition. *Proceedings of the IEEE*, 86(11):2278–2324, 1998.
- [27] Yann LeCun, Corinna Cortes, and Christopher JC Burges. The mnist database of handwritten digits, 1998.
- [28] Yann A LeCun, Léon Bottou, Genevieve B Orr, and Klaus-Robert Müller. Efficient backprop. In *Neural networks: Tricks of the trade*, pages 9–48. Springer, 2012.
- [29] Jason D Lee, Max Simchowitz, Michael I Jordan, and Benjamin Recht. Gradient descent converges to minimizers. *University of California, Berkeley*, 1050:16, 2016.
- [30] Mu Li, Tong Zhang, Yuqiang Chen, and Alexander J Smola. Efficient mini-batch training for stochastic optimization. In *Proceedings of the 20th ACM SIGKDD international conference on Knowledge discovery and data mining*, pages 661–670. ACM, 2014.
- [31] Long-Ji Lin. Reinforcement learning for robots using neural networks. Technical report, DTIC Document, 1993.
- [32] Volodymyr Mnih, Koray Kavukcuoglu, David Silver, Alex Graves, Ioannis Antonoglou, Daan Wierstra, and Martin Riedmiller. Playing atari with deep reinforcement learning. *arXiv preprint arXiv:1312.5602*, 2013.
- [33] Yuval Netzer, Tao Wang, Adam Coates, Alessandro Bissacco, Bo Wu, and Andrew Y Ng. Reading digits in natural images with unsupervised feature learning. 2011.
- [34] Daniel Povey, Arnab Ghoshal, Gilles Boulianne, Lukas Burget, Ondrej Glembek, Nagendra Goel, Mirko Hannemann, Petr Motlicek, Yanmin Qian, Petr Schwarz, et al. The kaldi speech recognition toolkit. In *IEEE 2011 workshop on automatic speech recognition and understanding*, number EPFL-CONF-192584. IEEE Signal Processing Society, 2011.
- [35] Benjamin Recht, Christopher Re, Stephen Wright, and Feng Niu. Hogwild: A lock-free approach to parallelizing stochastic gradient descent. In *Advances in Neural Information Processing Systems*, pages 693–701, 2011.
- [36] Uri Shaham, Yutaro Yamada, and Sahand Negahban. Understanding adversarial training: Increasing local stability of neural nets through robust optimization. *arXiv preprint arXiv:1511.05432*, 2015.
- [37] Karen Simonyan and Andrew Zisserman. Very deep convolutional networks for large-scale image recognition. *arXiv preprint arXiv:1409.1556*, 2014.
- [38] Daniel Soudry and Yair Carmon. No bad local minima: Data independent training error guarantees for multilayer neural networks. *arXiv preprint arXiv:1605.08361*, 2016.
- [39] Nitish Srivastava, Geoffrey E Hinton, Alex Krizhevsky, Ilya Sutskever, and Ruslan Salakhutdinov. Dropout: a simple way to prevent neural networks from overfitting. *Journal of Machine Learning Research*, 15(1):1929–1958, 2014.

- [40] Ju Sun, Qing Qu, and John Wright. When are nonconvex problems not scary? *arXiv preprint arXiv:1510.06096*, 2015.
- [41] I. Sutskever, J. Martens, G. Dahl, and G. Hinton. On the importance of initialization and momentum in deep learning. In *Proceedings of the 30th International Conference on Machine Learning (ICML 2013)*, pages 1139–1147, 2013.
- [42] O. Vinyals, A. Toshev, S. Bengio, and D. Erhan. Show and tell: A neural image caption generator. In *Proceedings of the IEEE Conference on Computer Vision and Pattern Recognition*, pages 3156–3164, 2015.
- [43] Sixin Zhang, Anna E Choromanska, and Yann LeCun. Deep learning with elastic averaging sgd. In *Advances in Neural Information Processing Systems*, pages 685–693, 2015.
- [44] Stephan Zheng, Yang Song, Thomas Leung, and Ian Goodfellow. Improving the robustness of deep neural networks via stability training. *arXiv preprint arXiv:1604.04326*, 2016.
- [45] Martin Zinkevich, Markus Weimer, Lihong Li, and Alex J Smola. Parallelized stochastic gradient descent. In *Advances in neural information processing systems*, pages 2595–2603, 2010.

A Details about Data Sets

We summarize the data sets used in our experiments in Table 7. The TIMIT data set is pre-processed using Kaldi [34] and trained using a fully-connected network. The rest of the data sets are used without any pre-processing.

Table 7: Data Sets

Data Set	Num. Data Points		Num. Features	Num. Classes	Modality	Reference
	Train	Test				
MNIST	60000	10000	28×28	10	Image	[26, 27]
TIMIT	721329	310621	360	1973	Speech	[13]
CIFAR-10	50000	10000	32×32	10	Image	[24]
CIFAR-100	50000	10000	32×32	100	Image	[24]

B Architecture of Networks

B.1 Network F_1

For this network, we use a 784-dimensional input layer followed by 5 batch-normalized [21] layers of 512 neurons each with ReLU activations. The output layer consists of 10 neurons with the softmax activation.

B.2 Network F_2

The network architecture for F_2 is similar to F_1 . We use a 360-dimensional input layer followed by 7 batch-normalized layers of 512 neurons with ReLU activation. The output layer consists of 1973 neurons with the softmax activation.

B.3 Networks C_1 and C_3

The C_1 network is a modified version of the popular AlexNet configuration [25]. For simplicity, denote a stack of n convolution layers of a filters and a Kernel size of $b \times c$ with stride length of d as $n \times [a, b, c, d]$. The C_1 configuration uses 2 sets of $[64, 5, 5, 2]$ -MaxPool(3) followed by 2 dense layers of sizes (384, 192) and finally, an output layer of size 10. We use batch-normalization for all layers and ReLU activations. We also use Dropout[39] of 0.5 retention probability for the two dense layers. The configuration C_3 is identical to C_1 except it uses 100 softmax outputs instead of 10.

B.4 Networks C_2 and C_4

The C_2 network is a modified version of the popular VGG configuration [37]. The C_3 network uses the configuration: $2 \times [64, 3, 3, 1]$, $2 \times [128, 3, 3, 1]$, $3 \times [256, 3, 3, 1]$, $3 \times [512, 3, 3, 1]$, $3 \times [512, 3, 3, 1]$ which a MaxPool(2) after each stack. This stack is followed by a 512-dimensional dense layer and finally, a 10-dimensional output layer. The activation and properties of each layer is as in B.3. As is the case with C_3 and C_1 , the configuration C_4 is identical to C_2 except that it uses 100 softmax outputs instead of 10.

C Performance Model

As mentioned in Section 1, a training algorithm that operates in the large-batch regime without causing a generalization gap has the ability to scale to much larger number of nodes than is currently possible. Further, it may also be possible to improve training time through faster convergence. We present an idealized performance model that demonstrates our goal.

For LB method to be competitive with SB method, the LB method must (i) converge to minima that generalizes, and (ii) do it in a reasonably low number of iterations, which we analyze here. Let I_s and I_ℓ be number of iterations it takes SB and LB methods to reach the point of comparable test accuracy, respectively. Let B_s and B_ℓ be corresponding batch sizes and P be number of processors being used for training. Assume that $P < B_\ell$, and let $f_s(P)$ be the parallel efficiency of the chosen SB method. For simplicity, we further assume that $f_\ell(P)$, the parallel efficiency of the LB method, is 1.0. In other words, we assume that the LB method is perfectly scalable due to large batch size.

For LB to be faster than SB, we want

$$I_\ell \frac{B_\ell}{P} < I_s \frac{B_s}{P f_s(P)}.$$

In other words, the ratio of iterations of LB to the iterations of SB should be

$$\frac{I_\ell}{I_s} < \frac{B_s}{f_s(P) B_\ell}.$$

For example, if $f_s(P) = 0.2$ and $B_s/B_\ell = 0.1$, the LB method must converge in at most half as many iterations as the SB method to see performance benefits. We refer the reader to [10] for a more detailed model and a commentary on the effect of batch-size on the performance.